Probing the Dynamics of Water in Chitosan Polymer Films by Dielectric Spectroscopy

P. Murugaraj, D. E. Mainwaring, D. C. Tonkin, M. Al Kobaisi

School of Applied Sciences, College of Science, Engineering and Health, Royal Melbourne Institute of Technology, Melbourne 3001, Australia

Received 2 August 2010; accepted 9 August 2010
DOI 10.1002/app.33163
Published online 23 November 2010 in Wiley Online Library (wileyonlinelibrary.com).

ABSTRACT: Chitosan biopolymers are increasingly being used in advanced biomedical applications, where aqueous interactions profoundly influence their physical properties and also their *in vivo* biomolecular and cellular activity. Here, hydration of chitosan films is studied by dielectric spectroscopy in a conventional constraining plate configuration and compared with free standing films. Film hydration proceeds by an initial water uptake followed by a spontaneous dehydration (deswelling) even in saturated atmospheres. At water contents above a critical value, $\sim$ 9.5 wt % a dielectric loss resonance peak (β_{wet}) arises from relaxation of evolving chitosan–water complexes, below this value insufficient interchain space for oscillation of these complexes prevents β_{wet} appearing. The β_{wet} frequency was related to water content by a power law with the frequency changing by $\sim$ 3 orders of magnitude. Importantly the scaling exponents (slopes) differed significantly for unconstrained (free standing) and volume constrained films indicating the effect of internal stresses in constrained films. Both dielectric and conductivity behavior were influenced by internal constraining stresses affecting both oscillatory motion and charge mobility. In biomedical devices, biopolymers may be free standing, surface adhered, or enclosed structures imposing different internal stresses on polymer chains and the mobility of their segments. Dielectric spectroscopy can examine these influences on dielectric and electrical characteristics, which play a critical role in biomolecular interactions. © 2010 Wiley Periodicals, Inc. J Appl Polym Sci 120: 1307–1315, 2011

Key words: biopolymers; chitosan; dielectric properties; spontaneous deswelling; conducting polymers

INTRODUCTION

The poly(aminosaccharide) chitosan, (1→4)-2-amino-2-deoxy-(D-glucose), is the N-deacetylated derivative of natural chitin. Chitosan shares the β-(1→ 4) linked glucopyranose residues with cellulose. Next to cellulose, chitin represents the second most abundant polysaccharide biopolymer. Chitosan is increasingly being used in advanced biomedical applications, such as drug delivery, tissue engineering scaffolds, wound dressings, skin graft templates, hemostatic agents, and hemodialysis membranes as well as general advanced technologies such as ionic conductors. As a biomaterial, chitosan has excellent mechanical strength, biocompatibility, and nontoxicity.[1,2] Recently, a novel etched composite scaffold of chitosan-gelatin reinforced by a poly(lactic-co-glycolic acid) (PLGA) membrane has been explored for its cell growth and mechanical stress relaxation.[2]

The dielectric properties of polysaccharides, carrying two hydroxyl groups and one methylol group, have been widely investigated in the past.[3,4] Dielectric relaxation spectroscopy probes the chain dynamics in polymers, separating contributions from different molecular groups of a repeating unit with respect to the rates of their orientation dynamics.[5]

Many modes of relaxation in dielectric spectroscopy have been reported for polysaccharides and their derivatives to occur over wide ranges of frequency and temperature. α relaxation represents the major dielectric relaxation in materials with permanent dipoles where its origin lies in segmental motions. Whereas β relaxation is the main process found in all polysaccharides at low temperatures (−135°C to +20°C) being related to segmental motion of the chains via the glucosidic bond, and therefore, it corresponds to local chain dynamics appearing just above 10^6 Hz. Thus, α and β relaxations have different molecular length scales although interrelated because the same dipoles usually contribute to both processes, hence β_{wet} relaxations merge at high temperature (and high frequency) to give rise to an αβ process.[6,7] Polysaccharides containing low levels of residual water show an additional relaxation

Correspondence to: P. Murugaraj (pandiyan.murugaraj@rmit.edu.au).

Contract grant sponsors: Australian Cooperative Research Centre for Polymers (CRC-P) (Chitosan Chemistry Program).

process termed β_{wet} relaxation. At present, there is no detailed molecular interpretation of this β_{wet} process although it relates to the motion of larger polymer–water complexes in a gel-like domain. At higher water contents, the β_{wet} relaxation process shifts to higher frequencies and the two processes of the β and β_{wet} merge into a common inseparable relaxation process in the dielectric spectra.[5]

Dielectric spectroscopy and other techniques such as differential scanning calorimetry (DSC) have also been used to identify the impact of the various types of water on polysaccharides particularly cellulose. Chitosan hydrogels, like other hydrogels, can have significant water contents, comprising water tightly bound to the polymer chains, which may freeze with a transition temperature below that of bulk water, further bound water that is nonfreezing[8–11] and free water. Water within chitosan films plays a pivotal role in establishing their molecular conformations. At low-water concentrations, chitosan chains forming extended twofold helices are stabilized by intramolecular hydrogen bonds including the stabilizing water molecules between chitosan sheets formed by these chains.[12–14] Importantly, Ogawa identified the details of the spontaneous transformations that occur between chitosan polymorphs whereby an anhydrous (annealed) chitosan polymorph forms with time even in the presence of humid or aqueous environments. Ferreira et al. subsequently detailed the initial molecular interactions between the chitosan chains and water molecules at nanoscale dimensions using molecular dynamics, and showed that the extent of hydrogen bond formation and disruption or rearrangement influenced the interchain free volume.[15] Increased water content gives rise to liquid crystalline mesophases and three-dimensional hydrogel networks.[16] The dynamics of swelling and deswelling of these chitosan structures also depend on pH and the degree of chain cross-linking, which have been exploited to achieve a range of hydrogel formation, drug release, and biodegradability characteristics.[17]

Most biopolymers are insulators because of a lack of free charge carriers. Their conductivity depends on the thermally generated carriers together with the addition of suitable dopants.[18,19] Chitosan films contain several polar groups such as $-OH$ and $-NH_2$, which can act as electron donors.[2] Understanding the charge transport behavior is receiving increased research attention due to its impact on its *in vivo* behavior in tissue engineering and scaffold applications. These films have been shown to be good ionic conductors when formed as chitosan-salt composites where the AC conductivity was shown to arise from the presence of mobile ions and charge carriers.[20–22] Most electrical conductivity studies have focused on salt based composite systems with very few addressing the intrinsic conductivity of chitosan biopolymer systems[23] where there appears to be no systematic studies of this intrinsic behavior.

In this work, we systematically study the dielectric relaxation phenomena associated with the onset and progress of chitosan hydration as both free standing films and films constrained volumetrically by the conventional parallel plate geometry adopted for such measurements. The arrangement adopted allowed measurements under controlled vapor conditions, which identified the spontaneous deswelling arising from expulsion of water during structural rearrangement. The arrangement also allowed the simultaneous measurement of charge transport properties, which evolved during hydration and dielectric relaxation.

EXPERIMENTAL

Chitosan (Sigma–Aldrich) had a degree of deacetylation of about 80% as determined by Fourier transform infrared spectroscopy (FTIR) and an average molecular weight 164 kDa. Chitosan films were fabricated by solution casting from 1% acetic acid, which was filtered through 0.45 μm syringe filters before casting on clean flat polystyrene Petri dish plates. The solvent was allowed to completely evaporate under ambient conditions. The resulting film was then washed thoroughly with 5% ammonia solution to neutralize residual acetic acid followed by washing with deionized water. The film was then rinsed with acetone followed by heat treatment in a vacuum oven at 100°C for 5 h to produce a dry chitosan film. Chitosan films produced had thicknesses between 30 and 70 μm, which were measured to ± 0.5 μm.

Two identical chitosan thin-film samples, produced from the same initial film of thickness 30 μm, were prepared with diameters of 12 mm and sputter coated with deposited gold as electrodes on both sides. Although one of the samples (Sample S1) was clamped between the parallel condenser plates for continuous monitoring of its dielectric properties under varying relative humidity conditions, the other sample (Sample S2) was placed under identical clamped conditions to monitor the corresponding weight changes arising from hydration.

A similar pair of chitosan films were produced at a thickness of 70 μm to allow equivalent dielectric measurements to be made on free standing films (unclamped films Sample S3 and Sample S4). Sample 3 was provided with flexible silver epoxy contacts of a similar size to the gold electrodes incorporating multistrand copper wire leads. Sample S4 was the equivalent reference film used for hydration monitoring. Moisture contents of the control film samples were monitored from weight changes immediately on removing from the humidity chamber to an accuracy of 0.0001 g.

Fourier transform infrared spectroscopy-attenuated total reflectance (FTIR-ATR) measurements in attenuated total reflectance mode (Spectrum 100, PerkinElmer) were carried out with universal diamond ATR top plate accessory. The scanning range was from 4000 to 550 cm^{-1} with a resolution of 2 cm^{-1} and 8 scans for each spectrum.

Dielectric spectroscopic measurements were made on these films in a parallel plate condenser mode configuration with a plate diameter of 12 mm similar to Bian and Mijovic[24] over the frequency range 10^1 to 10^6 Hz using a Hewlett-Packard low-frequency impedance analyser (HP 4192A) with samples within a humidity chamber under controlled relative humidity conditions at a constant temperature of 300°K. The signal amplitude was maintained at 1 V_{rms} throughout the measurements. The measured capacitance was in the range 10 pF to 1 nF for chitosan films with water content below 8.54 wt % and from 1 nF to 1 μF for films with water content between 9 and 40 wt %. The accuracy of the measured capacitance was ±0.01 pF for low-water content samples and ±1 pf for high-water content samples.

The frequency variation of capacitance and the dissipation factor of the films were measured in a series circuit mode and the dielectric parameters such as dielectric permittivity and dielectric loss were evaluated. The dielectric permittivity $\varepsilon'(\omega)$ is given by $C(\omega)/C_o$ where $C(\omega)$ is the capacitance measured at a frequency ω and C_o is the equivalent capacitance in air. Dielectric loss, a measure of energy loss which is a material property independent of sample geometry, is expressed as the loss tangent (tan δ) or dissipation factor and has contribution both from dipole relaxation and from dc conductivity, i.e., $\tan\delta = \varepsilon''/\varepsilon' + \sigma/2\pi f\varepsilon'$, where ε' and ε'' are real and imaginary components of the complex permittivity of the material, σ is the bulk dc conductivity of the films, and f is the measurement frequency.[25,26] The frequency dependence of the film impedance, in terms of their resistance and reactance (imaginary part of the resistance), was measured and the bulk DC conductivity (σ) was extracted from the Nyquist impedance plot. Data analysis was performed in terms of equivalent circuits using the algorithm of Boukamp[27] using nonlinear least square fitting. Subsequently, the dielectric loss, ε'', was corrected for the conductivity component using the expression above.

RESULTS AND DISCUSSION

Film hydration

Hydration of the clamped control films (S2 and S4) under saturated humidity was monitored as a function of time. Films with gold sputtered electrodes gained water that reached 8.54 wt % after 300 min and reached a maximum value of 18.09 wt % after a total time of 15 h. After this time, the water content in the S2 chitosan film decreased spontaneously in spite of the film being maintained at 100% relative humidity (RH) due to deswelling processes. The final water content appeared to stabilize at 11.23 wt % after 150 h as shown in Figure 4(inset). In contrast, similar weight gain measurements of the unclamped film (S4) showed a moisture gain of 40.42 wt %, i.e., more than twice that of the volume constrained film. After deswelling, the water content of this sample stabilized at 26.52 wt %.

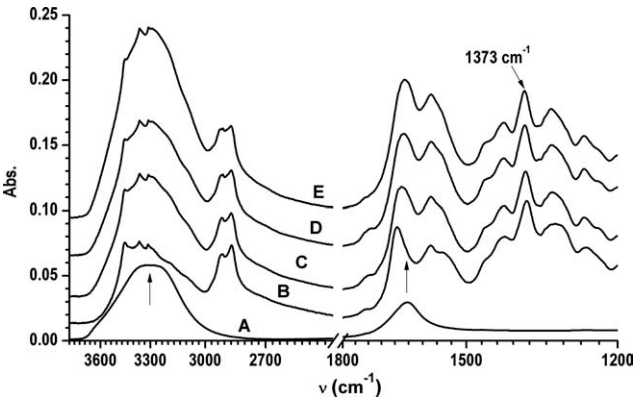

Figure 1 FTIR spectra of (A) water, (B) dry chitosan film, and (C—E) chitosan films with water contents 8.5, 16.0, and 30.0 wt %, respectively (spectra are normalized to the band at 1373 cm^{-1}, which was unaffected by the presence of water).

FTIR analysis

Figure 1 shows the FTIR spectra of chitosan films at various stages of water uptake. The dry chitosan film has absorption bands in the 3700–3000 cm^{-1} frequency range arising from amine and amide NH, and OH stretching bands and in the 1480–1750 cm^{-1} range arising from carbonyl stretching of secondary amides (amide I band), N—H bending vibrations of nonacylated 2-aminoglucose primary amines, and N—H bending vibrations of secondary amides (amide II band) bands.[28] The presence of swelling water in chitosan film increases the absorption in the frequency ranges (a) 3700–3000 cm^{-1} where pure liquid water has a broad absorbance band consisting of a symmetric stretching band ν1 at 3277 cm^{-1} and asymmetric stretching band ν3 at 3490 cm^{-1} and (b) 1480–1750 cm^{-1} where it has a bending band ν2 at 1643 cm^{-1}.[29] Although these bands may slightly shift or broaden due to new types of hydrogen bonding in the swollen chitosan environment, they can be used as indicative of water uptake by the polymer compared with dry polymers' spectrum.[30]

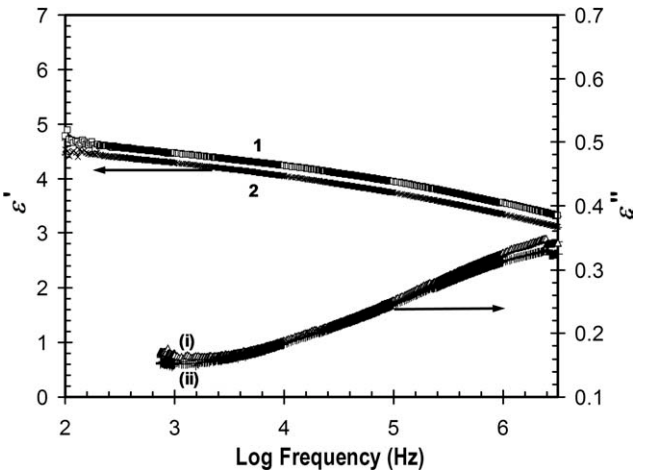

Figure 2 Frequency dispersion of dielectric permittivity and dielectric loss of dried (1, i) constrained and (2, ii) unconstrained chitosan films.

Dielectric spectroscopy

Dry chitosan films

Figure 2 shows a typical frequency dependent dielectric characteristics of the dry chitosan films in the S1 (clamped) and S3 (unclamped) configurations indicating that both electrode configurations produce identical dielectric responses. The DC conductivity was $<10^{-11}$ S/cm and the dielectric permittivity (ε') at 1 MHz for these films was 3.3 ± 0.1, consistent with values reported for a range of similar biopolymer matrices.[31] The low-frequency dielectric permittivity (ε') was about 4.4 ± 0.1 (at 100 Hz) indicative of negligible space charge contributions, whereas the dielectric loss corrected for DC loss (ε'') was ~ 0.16 at low frequencies increasing to 0.33 ± 0.01 at 1 MHz confirming the minimum effect of the of mobile charge carriers such as acetate ions or OH^- in these well-dried films.

Dielectric spectra of constrained films

Figure 3 shows the frequency dispersion of the dielectric permittivity (ε') and the dielectric loss (ε'') for the chitosan film S1 during progressive hydration in the humidity chamber. Up to an initial water uptake of 8.54 wt %, the ε' and ε'' at low frequencies increased steadily more than an order of magnitude with increasing water uptake. This behavior was similar to that reported in the literature for various systems such as polyethylene oxide containing hydrogen ions[32] and nanoporous silica containing water.[33] Figure 3 shows no development of a resonance peak in the dielectric loss (ε'') observed in the measured frequency range even after dc conductivity correction, indicative of the measured dielectric loss having high contributions from other dielectric relaxation processes in addition to the orientational dipolar relaxation. This high-dielectric loss in the low-frequency range arises from relaxation of the low-mobility charge carriers, namely, hydroxide ions. Such a high-dielectric loss may mask the α relaxation observed by Gonzalez-Campos et al.[34] at frequencies below 100 Hz for chitosan films. The increased low-frequency dielectric permittivity (which is not affected by the dc conductivity) also confirms the increasing formation of charged species with increasing hydration that contribute to the space charge polarization component (Maxwell-Wagner-Silliars) of the dielectric permittivity. The dielectric permittivity (ε') of this film at 1 MHz increased from 3.30 for the dry film to 5.56 for the film containing 8.54 wt % water, whereas the dielectric loss (ε'') exhibited only a marginal increase from 0.32 to 0.54 at this frequency.

When the water uptake is above 9 wt %, a dielectric loss resonance peak appeared above 500 Hz, in addition to the increased dielectric loss at low frequencies. The resonance peak appeared at a frequency of 510 Hz for a water content of 9.57 wt %, which then shifted to higher frequencies with increases in water uptake (Fig. 4). The high increase in the low frequency in the dielectric loss exhibits considerable overlap with the dielectric relaxation peak hence the dielectric loss factor ($\varepsilon''/\varepsilon'$) in Figure 4(inset) is plotted for improved clarity of the relaxation peaks. Under volume constrained conditions (S1), the resonance peak position was at 4 kHz at the maximum water uptake of 18.09 wt %. This peak can be identified with the β_{wet} relaxation resulting from the formation of bound chitosan–water complexes similar to those reported for polysaccharides by Einfeldt et al.[35] The shift of this peak position to higher frequencies with increasing water content is also consistent with the water dependency of these types of biopolymer–water complexes. Beyond this maximum uptake, a deswelling process with

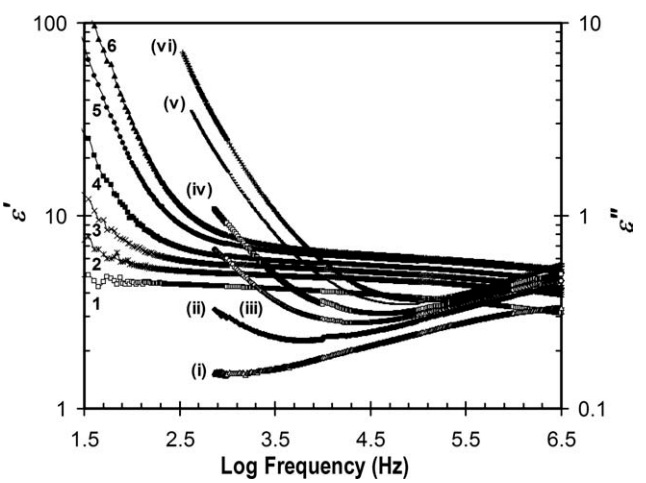

Figure 3 The dielectric permittivity (1–6) and dielectric loss (i–vi) of a constrained chitosan film with the specific water contents: 0, 3.1, 4.5, 5.3, 7.1, and 8.54 wt %.

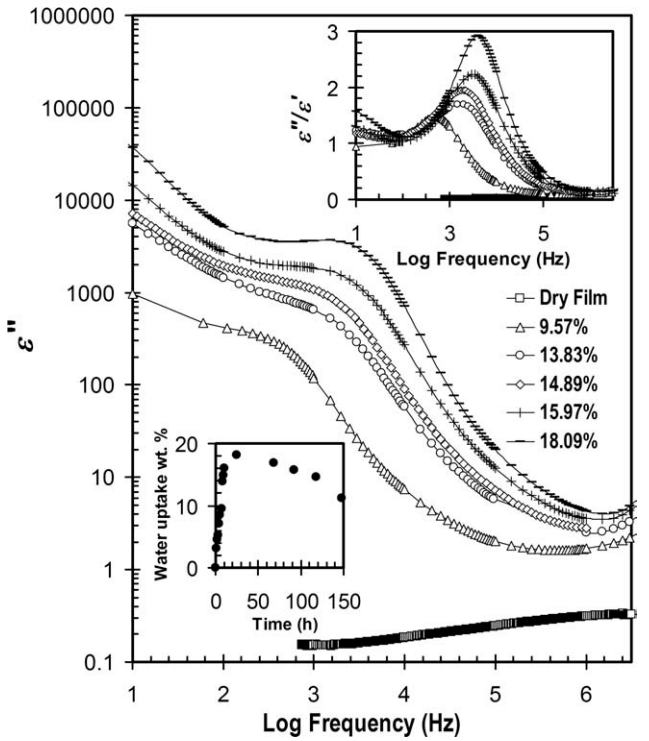

Figure 4 The dielectric loss of a constrained chitosan film with increasing water content.

concomitant expulsion of water occurs (Fig. 4, inset), which is also reflected in the measured dielectric characteristics by the shift of dielectric loss resonance peak to lower frequencies (Fig. 5).

It is notable that this relaxation is not observable during the initial stages of hydration of a dry chitosan film [<9 wt %, Fig. 4(inset)], which may reflect the lack of sufficient interchain free space in the relaxing matrix for the dipoles to undergo oscillation due to limited swelling of chitosan in the initial stages.

As noted, during increasing hydration from the dry chitosan state, the dielectric loss peak not only shifted to higher frequencies but also increased in intensity (Fig. 4), indicative of an increased concentration and strength of the oscillating dipole relaxation. During the deswelling process (Fig. 5), the dielectric loss peak moved to lower frequencies with decreasing water content but increased in magnitude. That is, the frequency dependence of the dielectric loss peak follows the hydration–dehydration (spontaneous deswelling) cycle but the magnitude continues to increase across these hydration–dehydration processes. Here it can be seen that the dielectric behavior, in terms of the β_{wet} resonance peak arising from the relaxation of the evolving water–chitosan complexes (polar chain side groups and bound water), is sensitive to both the hydration and spontaneous deswelling processes. This overall behavior is consistent with the single crystal studies of Okuyama et al.[14] who detailed complete spontaneous dehydration of chitosan in saturated water environment at both elevated and ambient temperatures. Figure 5 shows that these chitosan films did not undergo complete dehydration because they consist of semicrystalline regions and disordered chitosan hydrogel unlike their single crystal counterparts. Dehydration that occurred during deswelling reduced the water content to 11.24 wt % compared with a calculated value of 10.62 wt %, which corresponds to 1 water molecule for each glucosamine in the 80% deacetylated chitosan. The bound water–chitosan complexes in the crystalline regions are illustrated diagrammatically in Figure 6. Water molecules form bridges between chitosan chains stabilizing the crystal structure. These constitute the non-freezing bound water within the structure, which characteristically changes the relaxation processes due to increased cooperative motion of local chains as reflected in their measured dielectric properties.

Dielectric loss spectra of free standing films.

Similar hydration and simultaneous dielectric measurements carried out on unclamped films (S3 and S4) showed that when the water content rose to 40.42 wt % having the volume unconstrained, the corresponding dielectric relaxation peak at this maximum hydration was 126 kHz. Spontaneous deswelling subsequently reduced the water content of this

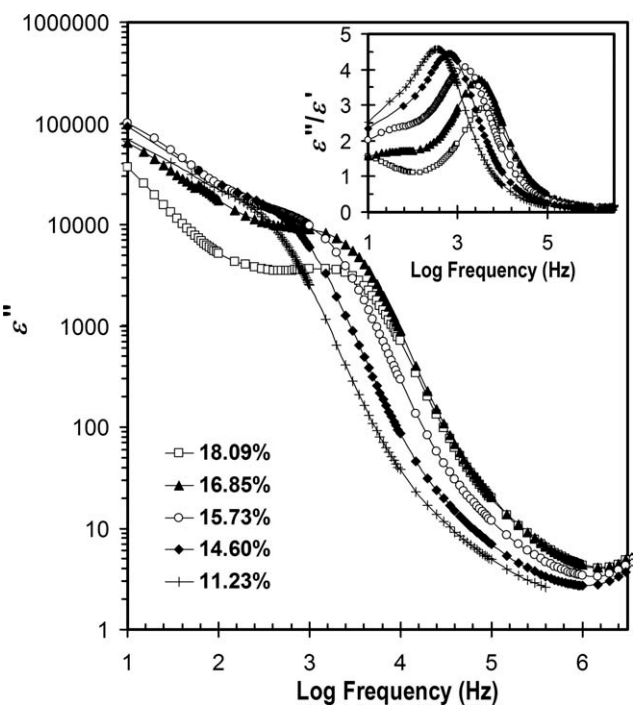

Figure 5 The dielectric loss of the constrained chitosan film during the deswelling process.

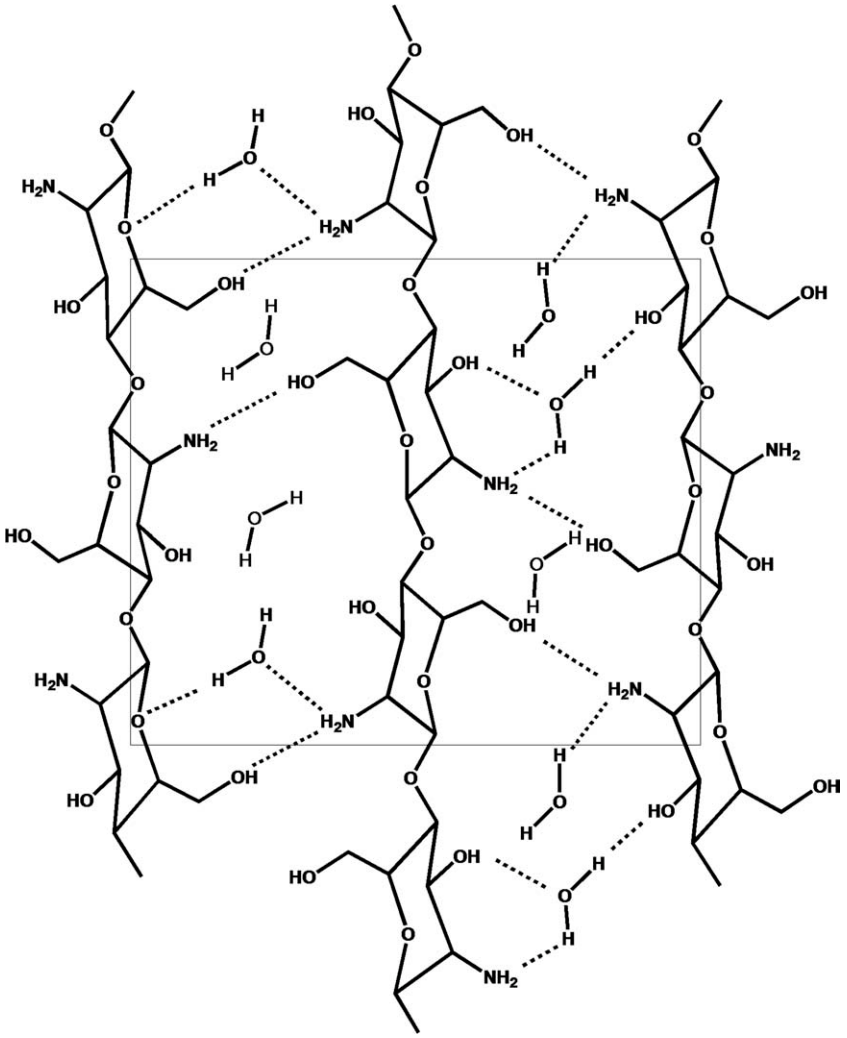

Figure 6 Representation of the water-chitosan chain complexes in the crystalline regions of the films.

film to a stable value of 26.52 wt %, which was accompanied by shift of the dielectric loss peak back to 25.26 kHz.

Figure 7 shows the relationship of the dielectric relaxation peak to the water content for the free standing and constrained films. Here, it can be seen that both film conditions fit power law behavior to very high degrees ($R^2 = 0.999$ and 0.974) over the water content range where a dielectric resonance loss peak appears. As noted, below these water contents, there appears insufficient interchain space for oscillating mobility of these complexes. These systems give scaling exponents of 2.97 and 3.88 for the unconstrained and constrained films, respectively, indicative of the increased effect of internal stresses in the volume constrained films. During spontaneous deswelling, the corresponding peak positions for equivalent water contents were always lower than the water uptake branch, indicative of irreversible chain orientation during water expulsion at 300 K leading to greater ordering and chain mobility.

Dielectric permittivity of hydrated films

Figure 8 shows the frequency dependence (dispersion) of the dielectric permittivity (ε') for the volume constrained chitosan film (S1) with water contents above 9.6 wt %. In timescales up to 500 Hz, the dielectric permittivity has a major contribution from Maxwell-Wagner-Sillars relaxation processes (e.g., interfacial space charge polarization arising from mobile OH^- ions), whereas the dielectric contribution in the frequency range from 500 Hz to 5 MHz arises from the relaxation of the water–chitosan complexes. In this region, the ε' increased progressively with water content for both the constrained and free standing films.

Figure 9 shows the dielectric permittivity at 1 MHz with increasing water content. As noted, the 1 MHz region represents solely dipolar contributions from hydrated chitosan complexes, which have two major components. The unbound water having a high dipole moment and a dielectric permittivity of 80 follows the Maxwell-Wagner mixing rule as

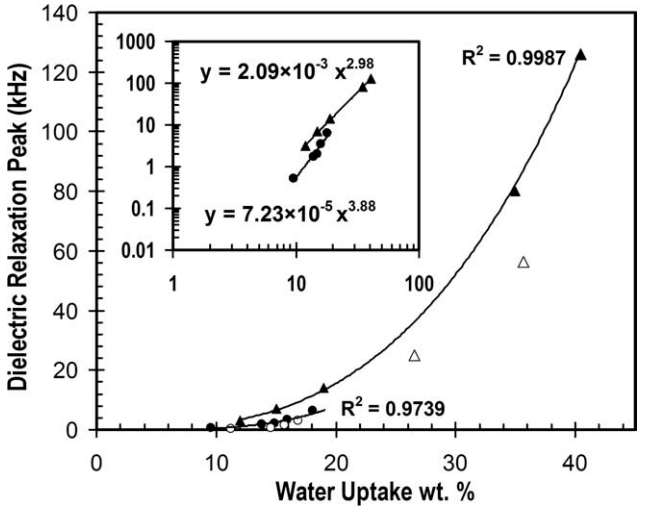

Figure 7 Shift of the dielectric loss resonance peak position with water content in unconstrained (△) and volume constrained (●) chitosan films. Open symbols are resonance peak shift during spontaneous deswelling process. Inset represents the log plot.

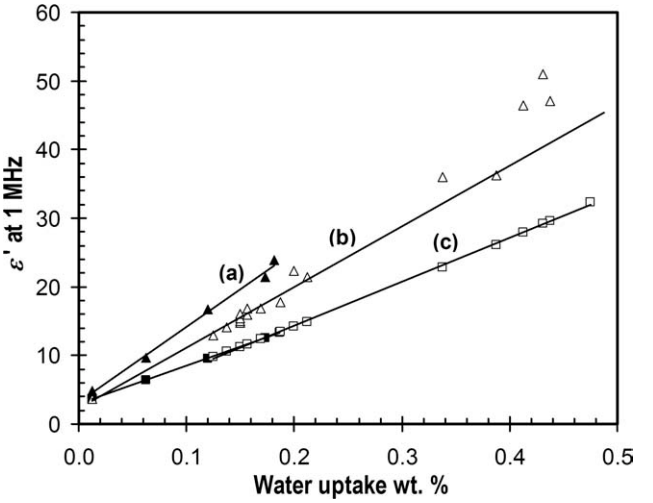

Figure 9 Dielectric permittivity (at 1 MHz) of chitosan films: (a) constrained, (b) free standing, and (c) Maxwell-Wagner's mixture rule.

shown in Figure 9(c). Here, it can be seen that all unbound water accounts for only part of the dielectric enhancement indicating the remainder arises from orientation of the intrinsic dipolar water–chitosan complex itself.

Figure 9 also shows the dielectric permittivity of the volume constrained film. For given water content, the dielectric permittivity of the volume constrained film was consistently higher than the free standing film, whereas the dielectric relaxation peak appeared at lower values as compared with free standing film (Fig. 7). As noted, this arises from differences in the internal stresses impacting on chain dynamics which may also alter the ratio of bound and free water in the constrained and free standing films.

Impedance of hydrated chitosan films.

The frequency dependence of the film impedance, in terms of their resistance and reactance (imaginary part of the resistance), was measured at various water contents and the bulk DC conductivity was extracted from the Nyquist impedance plot given in Figure 10.

The bulk electrical conductivity increased exponentially (Fig. 11) for both clamped and unclamped films over their respective water uptake ranges. When the water content of the free standing film increased from 11.25 to 40.42 wt % the electrical conductivity increased from 10^{-8} to 10^{-5} S/cm, which is consistent with the value reported by Wan et al.[23] for fully hydrated chitosan immersed in water. Significantly, the clamped film showed lower

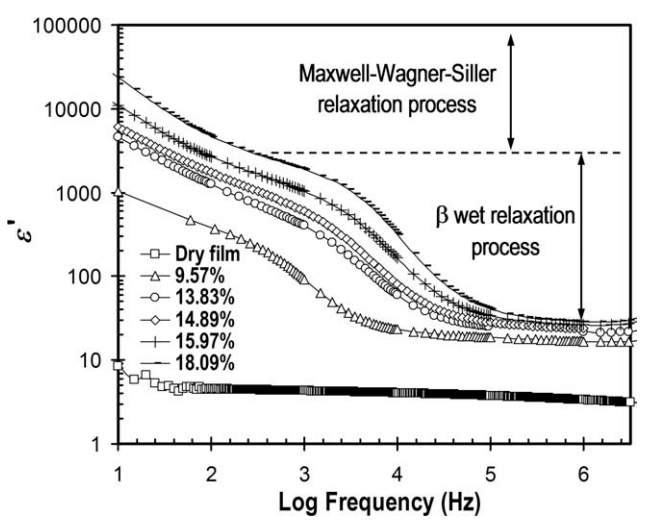

Figure 8 Typical frequency dispersion of the dielectric permittivity of the constrained chitosan film with varying water content.

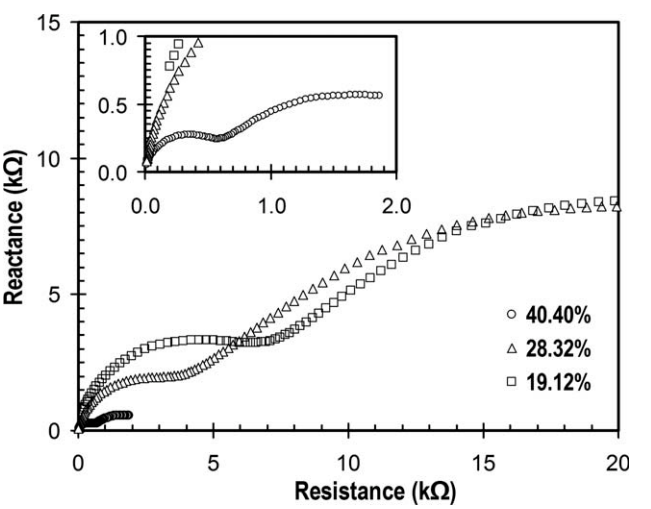

Figure 10 Nyquist plot of resistance (R) and reactance (-X) for a free standing chitosan film at three water contents.

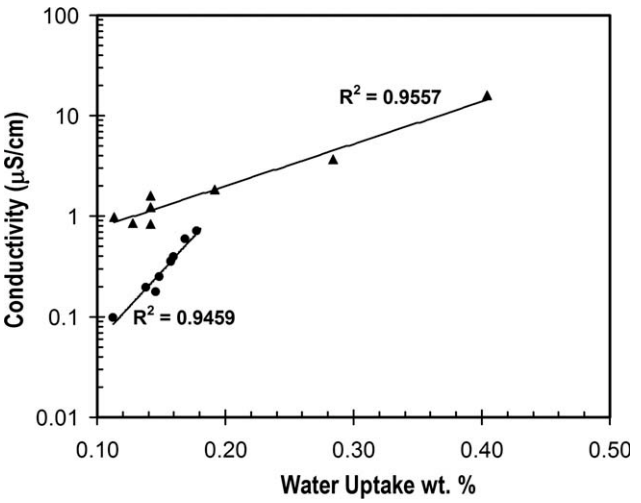

Figure 11 DC electrical conductivity of the unconstrained (▲) and volume constrained (●) chitosan films at different water contents.

conductivities, again influenced by the effects of internal constrained stresses which would affect the mobilities of the charged species in this biopolymer polyelectrolyte.

CONCLUSIONS

Here, we have studied the hydration processes in chitosan films in a volume constrained configuration between two parallel plate electrodes and compared it with free standing films having flexible electrode pads within a controlled humidity chamber using dielectric spectroscopy (10^1 to 10^6 Hz). These studies have shown that the hydration process in chitosan films proceeds with an initial uptake of water followed by spontaneous dehydration even in saturated water environments consistent with the single crystal work of Okuyama et al. at elevated and ambient temperatures.[14]

A dielectric loss resonance peak identified as a "β_{wet} resonance peak" appeared at 510 Hz for a water content of 9.57 wt % arising from relaxation of the evolving chitosan–water complexes (polar chain side groups and bound water) that was found to be sensitive to both the hydration and spontaneous deswelling processes. The frequency of this relaxation peak at differing water contents for the free standing and constrained films was found to fit a power law relationship with the peak frequency changing by about three orders of magnitude over the water content range where the β_{wet} peak appears. At lower water contents, there appears insufficient interchain space for oscillating mobility of the chitosan–water complexes to give a β_{wet} peak. The difference in scaling exponents ($\sim$ 3.0 and $\sim$ 3.4) for the unconstrained and constrained films, respectively, indicates the increased effect of internal stresses in volume constrained biopolymers.

The dielectric permittivity of the hydrated chitosan films increased more than predicted by the Maxwell–Wagner mixing rule indicative of enhancement from the formation of chitosan chain-bound water complexes adding to the contributions from dipole polarizabilities which reinforced the identity of the β_{wet} resonance peak.

The bulk electrical conductivity of the hydrated films increased from $<10^{-11}$ S/cm for the dry film to $>10^{-5}$ S/cm for the film with 40.42 wt % water. This conductivity originates from the relatively mobile OH^- ions of the bound water attaching to weakly basic NH_2 side groups during the hydration process. Thus, both dielectric behavior and electrical conductivity are influenced by internal constraining stresses affecting oscillations of the chitosan-water complexes and the mobilities of the charged species, respectively.

The use of biopolymers, such as chitosan, in biomedical devices may be in free standing, surface adhered or enclosed geometries. These environments impose a range of internal stresses on the polymer chain microstructure and the mobility of its chain segments. Dielectric spectroscopy is able to explore the influence of these stress fields on the chain dynamics under these various constraining conditions, together with its impact on their dielectric and electrical characteristics which was shown by Lima et al.[31] to critically affect biopolymer use in biomedical applications.

D.C.T. acknowledges receipt of a CRC-P PhD scholarship.

References

1. Ravi Kumar, M. N. V. React Funct Polym 2000, 46, 1.
2. Twu, Y.-K.; Chang, I. T.; Ping, C.-C. Carbohydr Polym 2005, 62, 113.
3. Crofton, D. J.; Pethrick, R. A. Polymer 1982, 23, 1609.
4. Boutros, S.; Hanna, A. A. J Polym Sci Polym Chem Ed 1978, 16, 89.
5. Einfeldt, J.; Kwasniewski, A.; Meißner, D.; Gruber, E.; Henricks, R. Macromol Mater Eng 2000, 283, 7.
6. Mijovic, J.; Andjelic, S.; Yee, C. F. W.; Bellucci, F.; Nicolais, L. Macromolecules 1995, 28, 2797.
7. Andjelic, S.; Fitz, B.; Mijovic, J. Macromolecules 1997, 30, 5239.
8. Bhaskar, G.; Ford, J. L.; Hollingsbee, D. A. Thermochim Acta 1998, 322, 153.
9. Agrawal, A. M.; Manek, R. V.; Kolling, W. M.; Neau, S. H. J Pharm Sci 2004, 93, 1766.
10. Capitani, D.; De Angelis, A. A.; Crescenzi, V.; Masci, G.; Segre, A. L. Carbohydr Polym 2001, 45, 245.
11. Liu, W. G.; Yao, K. D. Polymer 2001, 42, 3943.
12. Ogawa, K. J Met Mater Miner 2005, 15, 1.
13. Ogawa, K.; Yui, T.; Okuyama, K. Int J Biol Macromol 2004, 34, 1.
14. Okuyama, K.; Noguchi, K.; Kanenari, M.; Egawa, T.; Osawa, K.; Ogawa, K. Carbohydr Polym 2000, 41, 237.
15. Ferreira, M. L.; Pedroni, V. I.; Alimenti, G. A.; Gschaider, M. E.; Schulz, P. C. Colloids Surf A 2008, 315, 241.
16. Ratto, J.; Hatakeyama, T.; Blumstein, R. B. Polymer 1995, 36, 2915.

17. Li, Q.; Dunn, E. T.; Grandmaison, E. W.; Goosen, M. F. A. J Bioact Compat Polym 1992, 7, 370.
18. Mehendru, P. C.; Pathak, N. L.; Jain, K.; Mehendru, P. Phys Status Solidi A 1977, 42, 403.
19. Sinha, H. C.; Talwar, I. M.; Shrivastava, A. P. Thin Solid Films 1981, 82, 229.
20. Winie, T.; Majid, S. R.; Khiar, A. S. A.; Arof, A. K. Polym Adv Technol 2006, 17, 523.
21. Wan, Y.; Creber, K. A. M.; Peppley, B.; Bui, V. T. J Membr Sci 2006, 280, 666.
22. Lopez-Chavez, E.; Martinez-Magadan, J. M.; Oviedo-Roa, R.; Guzman, J.; Ramirez-Salgado, J.; Marin-Cruz, J. Polymer 2005, 46, 7519.
23. Wan, Y.; Creber, K. A. M.; Peppley, B.; Bui, V. T. Polymer 2003, 44, 1057.
24. Bian, Y.; Mijovic, J. Polymer 2009, 50, 1541.
25. Pethrick, R. A.; Hayward, D. Prog Polym Sci 2002, 27, 1983.
26. Lu, J.; Moon, K.-S.; Xu, J.; Wong, C. P. J Mater Chem 2006, 16, 1543.
27. Boukamp, B. A. Equivalent Circuit—EQUIVCRT Program-Users Manual, v3.97; University Twente: Holand, 1989.
28. Xu, J.; McCarthy, S. P.; Gross, R. A.; Kaplan, D. L. Macromolecules 1996, 29, 3435.
29. Max, J. J.; Chapados, C. J Chem Phys 2009, 131, 184505.
30. Nogales, A.; Ezquerra, T. A.; Rueda, D. R.; Martinez, F.; Retuert, J. Colloid Polym Sci 1997, 275, 419.
31. Lima, C. G. A.; de Oliveira, R. S.; Figueiró, S. D.; Wehmann, C. F.; Góes, J. C.; Sombra, A. S. B. Mater Chem Phys 2006, 99, 284.
32. Fanggao, C.; Saunders, G. A.; Lambson, G. F.; Hampton, R. N.; Carin, C.; Di Marco, C.; Lanza, M. J Polym Sci Part B: Polym Phys 1996, 34, 425.
33. Spanoudaki, T.; Albela, B.; Bonneviot, L.; Peyrard, M. Eur Phys J E 2005, 17, 21.
34. Gonzalez-Campos, J. B.; Prokhorov, E.; Luna-Barcenas, G. J Polym Sci Part B: Polym Phys 2009, 47, 2259.
35. Einfeldt, J.; Meißner, D.; Kwasniewski, A.; Einfeldt, L. Polymer 2001, 42, 7049.